17. M. D. Lewis, J. K. Cha, and Y. Kishi, *J. Am. Chem. Soc.*, **104**, 4976 (1982).
18. R. R. Schmidt and M. Hoffmann, *Tetrahedron Lett.*, **23**, 409 (1982).
19. R. A. Eade and H. P. Pham, *Aust. J. Chem.*, **32**, 2483 (1978).

Electronic Structures and Properties of the Charged Model Clusters Relating to High-T_c Superconductor $YBa_2Cu_3O_{7-x}$

U-Hyon Paek†*, Kee Hag Lee*, Yong Kiel Sung‡, and Wang Ro Lee

Department of Chemistry, WonKwang University, Iri 507-749
†Department of Chemistry, Gyeongsang National University, Jinju 660-701
‡Department of Chemistry, Dongguk University, Seoul 100-715. *Received March 15, 1991*

We have carried out an extended Hückel calculation to rationalize the role of CuO_3 chains and the size effect of the charged model clusters for the following charged model culsters: $Cu_6O_{21}^{28-}$, $Cu_6O_{22}^{30-}$, $Cu_9O_{30}^{39-}$, $Cu_9O_{32}^{43-}$, $Cu_{12}O_{38}^{48-}$, $Cu_{15}O_{50}^{65-}$, $Cu_{18}O_{54}^{66-}$, $Cu_{18}O_{55}^{68-}$, $Cu_{24}O_{70}^{84-}$, and $Cu_{27}O_{78}^{93-}$ for high -T_c superconductor $YBa_2Cu_3O_7$; $Cu_6O_{18}^{22-}$, $Cu_9O_{26}^{31-}$, $Cu_{12}O_{32}^{36-}$, $Cu_{15}O_{42}^{49-}$, $Cu_{18}O_{46}^{50-}$, $Cu_{24}O_{60}^{64-}$, and $Cu_{27}O_{66}^{69-}$ for insulator $YBa_2Cu_3O_6$. The results show that the electronic structures and properties of the charged model clusters relating to high-T_c superconductor are very sensitive to the size change of the clusters with various environmental effects, whereas those of the charged model clusters for insulator $YBa_2Cu_3O_6$ are monotonous to the size change. The CuO_3 chains along the *b*-direction may yield cooperative electronic coupling with the CuO_2 layers in determining both conducting and superconducting properties of $YBa_2Cu_3O_{7-x}$ system.

Introduction

The recent dramatic increases[1,2] of T_c have given reason to believe that some totally new mechanism for superconductivity is operating in the high-T_c superconductor, $YBa_2Cu_3O_{7-x}$. One significant conclusion about the new oxide superconductors is that there is a short coherence length for the electron pair.[3] Also sleight suggested this pair as existing in real space instead of momentum space.[4] In real space the structure of the high-T_c materials is very important. The structure of high-T_c superconductor, $YBa_2Cu_3O_{7-x}$, has been determined and confirmed by many different groups.[4-8] The distinct structural unit in $YBa_2Cu_3O_{7-x}$ superconducting system in Figure 1 contains 2 copper atoms (called Cu(2)) with a square pyramidal coordination by 5 oxygen atoms and 1 copper atom (called Cu(1)) with a square planar coordination by 4 oxygens. There are O(1)-Cu(1) chains along the *b*-direction. These chains and planes form a sub-lattice of repeating CuO_2-CuO_3-CuO_2 units along the *c*-direction. Magnetic rare-earth substitution studies[9] and the lack of copper-oxygen chains in the $(La_{1-x}M_x)_2CuO_{4-y}$ (M=Sr or Ba) superconducting system[10] led some to believe that the CuO_3 chains were responsible for the much higher transition temperatures in the new Y-Ba-Cu-O system. However, recent Zn and Ga substitution studies,[11] as well as the discovery of the $(AO)_m$-$ACa_{n-1}Cu_nO_{2n+2}$ phases[4,12] where A is Bi or Tl, indicate that the CuO_3 chains are not essential to high-temperature superconductivity. Their role is not yet clear.

One of the problems that make it difficult to study the high-T_c superconductor $YBa_2Cu_3O_{7-x}$ is that the single crystals,[13] which can now be routinely produced, are twinned. The twinned structure precludes the possibility of measurement to distinguish between the *a*- and *b*-directions that are particularly important in this system because of the on-going discussion as to where the CuO_3 chains along the *b*-direction play an important role in the superconducting process. It has recently become possible to detwin single crystals.[14] Recently a Brillouin scattering study[15] shows the anisotropy of the surface wave velocity in the *a*-*b* plane of an untwinned crystal but the isotropy of that in the *a*-*b* plane of twinned crystal. Band structure and cluster calculations of varying degrees of sophistication have been reviewed on the high-temperature oxide superconductors.[12b] In order to better understand the high-T_c superconductor $YBa_2Cu_3O_{7-x}$, it is important to correlate the structure with the physical properties of both superconducting $YBa_2Cu_3O_7$ and nonsuperconducting $YBa_2Cu_3O_6$. The purpose of this work is to understand whether the CuO_3 chains play any role in determining superconductivity, and to study the size effect of the model clusters along the *a*-, *b*-direction, and both the *a*- and *b*-directions.

We have carried out extended Hückel cluster calcula-

Table 1. Atomic Parameters Used in the Calculation[16]

	H_{ii} (eV)			Exponents		
	s	*p*	*d*	*s*	*p*	*d*
Cu	−11.4	−6.06	−14.0	2.2	2.2	5.9533(0.5933) 2.30(0.5744)
O	−32.3	−14.8		2.275	2.275	

*To whom correspondence should be addressed.

Table 2. Atomic Coordinates of $YBa_2Cu_3O_7$ and $YBa_2Cu_3O_6$

Atom	X/a	Y/b	Z/c[a]
Cu(1)	0.00	0.00	0.00
Cu(2)	0.00	0.00	0.3556
O(1)	0.00	0.50	0.00
O(2)	0.50	0.00	0.3773
O(3)	0.00	0.50	0.3789
O(4)	0.00	0.00	0.1584

[a] Beno *et al.*[5], (Argonne): $YBa_2Cu_3O_7$: $a=3.8231$, $b=3.8863$, $c=11.6807$ Å.

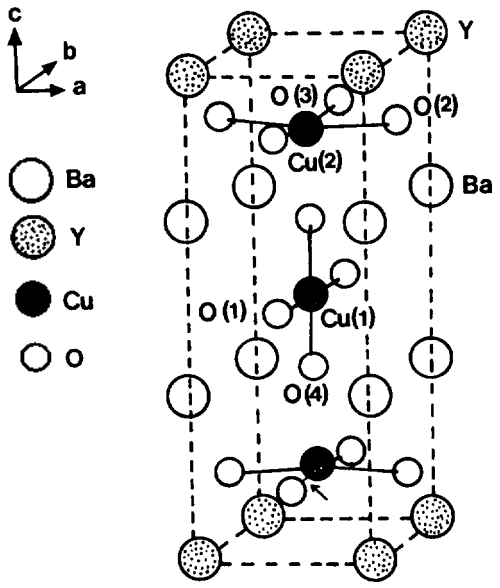

Figure 1. Unit cell of orthorhombic $YBa_2Cu_3O_7$ (ordered vacancy model), and $YBa_2Cu_3O_6$, the O(1) site is vacant.

tions[16,17] on the charged model clusters, with and without O(1) vacancy, to model O(1) vacancies in the Y-Ba-Cu-O systems as follows: $Cu_6O_{21}^{28-}$, $Cu_6O_{22}^{30-}$, $Cu_9O_{30}^{39-}$, $Cu_9O_{32}^{43-}$, $Cu_{12}O_{38}^{48-}$, $Cu_{15}O_{50}^{65-}$, $Cu_{18}O_{54}^{66-}$, $Cu_{18}O_{55}^{68-}$, $Cu_{24}O_{70}^{84-}$ and $Cu_{27}O_{78}^{93-}$ for high-T_c superconductor $YBa_2Cu_3O_7$; $Cu_6O_{18}^{22-}$, $Cu_9O_{26}^{31-}$, $Cu_{12}O_{32}^{36-}$, $Cu_{15}O_{42}^{49-}$, $Cu_{18}O_{46}^{50-}$, $Cu_{24}O_{60}^{64-}$, and $Cu_{27}O_{66}^{69-}$ for insulator $YBa_2Cu_3O_6$.

The atomic parameters[16] used in this study are summarized in Table 1.

Investigation of Electronic Structure and Properties

For orthorhombic $YBa_2Cu_3O_7$ and unrelaxed $YBa_2Cu_3O_6$, we use the atomic coordinates obtained by Beno *et al.*[5] as shown in Table 2. Here we choose the unrelaxed $YBa_2Cu_3O_6$ structure to determine whether the CuO_3 chains along the *b*-direction play any role in the superconducting process.

The hypothetical clusters[17] (*a* and *b*) shown in Figure 2 are taken to be our models for the calculations of $YBa_2Cu_3O_7$ and $YBa_2Cu_3O_6$, respectively. The Y and Ba cations are not included, since while the Y cations separate the two sets of CuO_2 layers, the Ba cations form Ba-O(4) planes that do

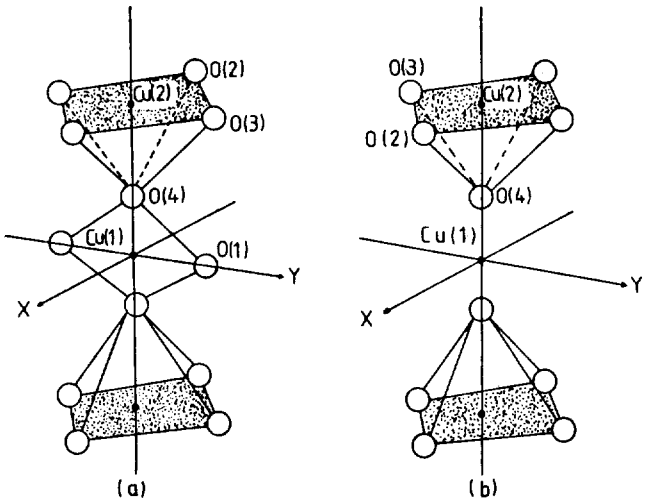

Figure 2. (a) Local environment for the Cu(1) and Cu(2) atoms in the unit charged model cluster representing the unit cell of $YBa_2Cu_3O_7$. (b) Local environment for the Cu(1) and Cu(2) atoms in the unit charged model cluster representing the unit cell of $YBa_2Cu_3O_6$.

not affect significantly the energy levels of the CuO_2 layers and the CuO_3 chains. Massida *et al.*[18] have considered that the Y and Ba atoms form an ordered superlattice structure and the O vacancies appear to play a crucial role in stabilizing the high-T_c superconductor $YBa_2Cu_3O_{7-x}$.

Schematic representations of the charged model clusters, which are the perspective drawing along the *a*-direction, showing the links between the Cu coordination polyhedra, are as follows:

(a) for the charged model clusters representing superconductor $YBa_2Cu_3O_7$. $Cu_3O_{12}^{17-}$, **1a**; $Cu_6O_{21}^{28-}$, **2.1a**; $Cu_6O_{22}^{30-}$, **2.2a**; $Cu_9O_{30}^{39-}$, **3.1a**; $Cu_9O_{32}^{43-}$, **3.2a**; $Cu_{12}O_{38}^{48-}$, **4a**; $Cu_{15}O_{50}^{65-}$, **5a**; $Cu_{18}O_{54}^{66-}$, **6.1a**; $Cu_{18}O_{55}^{68-}$, **6.2a**; $Cu_{24}O_{70}^{84-}$, **8.1a**; and $Cu_{27}O_{78}^{93-}$, **9a**.

(b) for the charged model clusters representing insulator $YBa_2Cu_3O_6$. $Cu_3O_{10}^{13-}$, **1b**; $Cu_6O_{18}^{22-}$, **2.1b**, **2.2b**; $Cu_9O_{26}^{31-}$, **3.1b**, **3.2b**; $Cu_{12}O_{32}^{36-}$, **4b**; $Cu_{15}O_{42}^{49-}$, **5b**; $Cu_{18}O_{46}^{50-}$, **6.1b**, **6.2b**; $Cu_{24}O_{60}^{64-}$, **8.1b**; and $Cu_{27}O_{66}^{69-}$, **9b**.

Here we choose the nominal charges of each ion as follows: +7 for Cu_3 ions; +3 for Y ions; +2 for Ba ions; and −2 for O ions.

The molecular orbital energy level diagrams as shown in Figures 3 and 4 reveal a difference between the electronic structures of **1a-9a** and **1b-9b**, with and without the CuO_3 chains, respectively. Variations of highest-energy occupied levels on the charged model clusters representing the superconductor $YBa_2Cu_3O_7$ shown in Figure 3 are jagged within the energy of 0.108 eV. This energy is dependent upon the sizes of the charged model clusters along the *a*-, *b*-, and both the *a*- and *b*-directions. Those on the charged model clusters representing the insulator $YBa_2Cu_3O_6$ shown in Figure 4 monotonously increase within 0.047 eV with the increment of the size of charged model clusters.

Figure 5 shows that the band gap between the bottom of the cluster z^2-y^2 Cu(1) band and the top of the cluster x^2-y^2 Cu(2) band for the charged model clusters representing $YBa_2Cu_3O_7$ decreases with increasing the size of the CuO_3

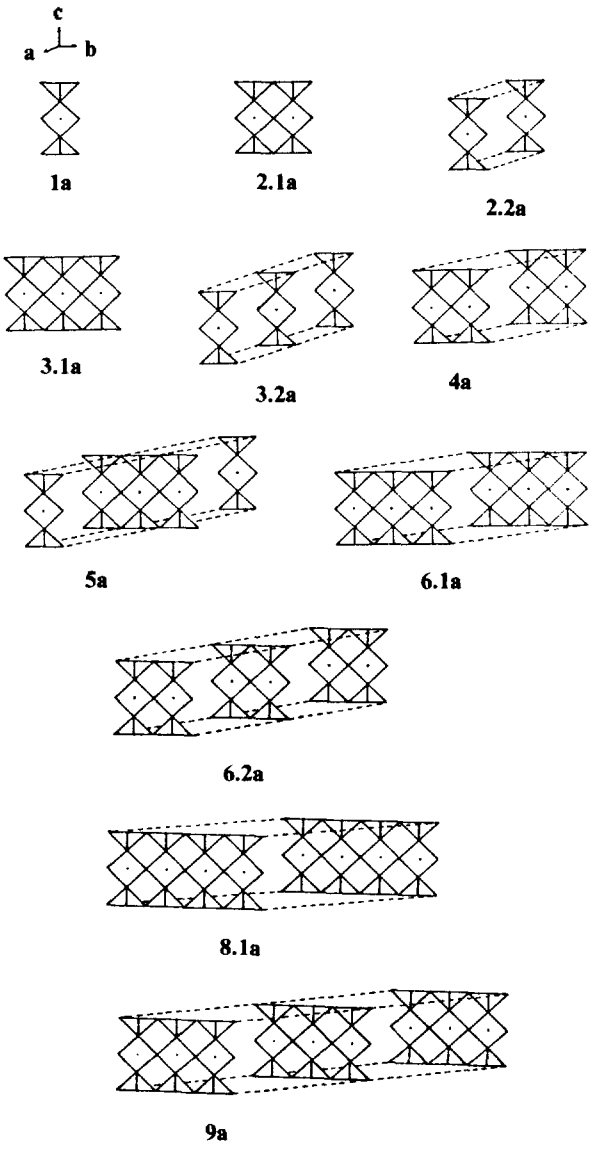

Scheme 1.

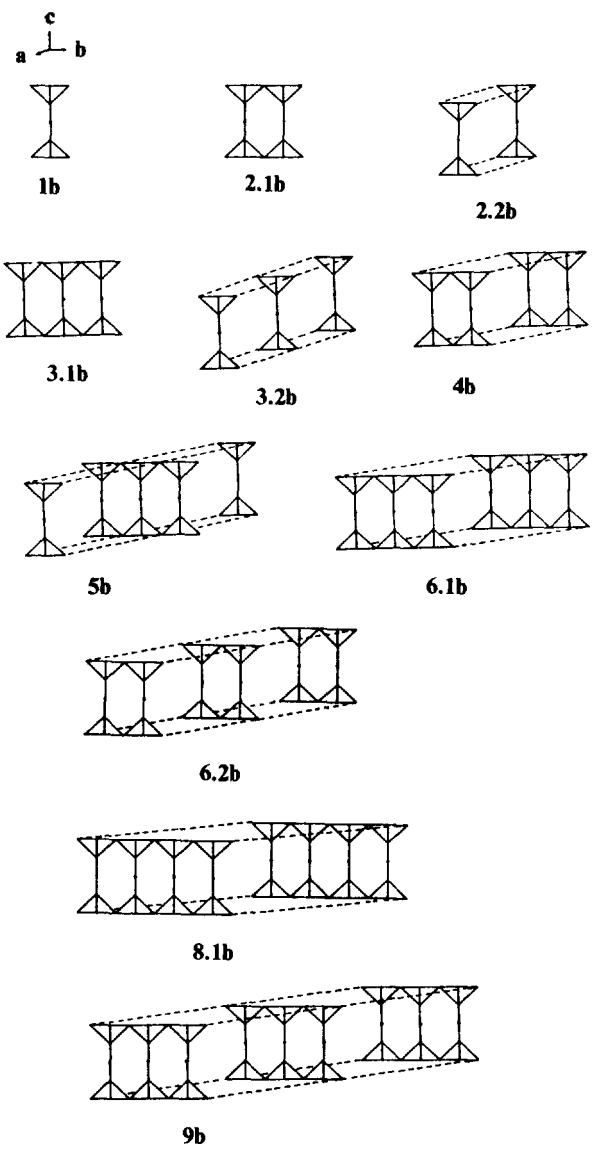

Scheme 2.

chains from one unit to three units along the *b*-direction. The increasing effect of one unit of the CuO_3 chains from **1a** to **4a** along the *a*- or/and *b*-directions is larger than that of CuO_3 chains from **4a** to **6.1a**. Each band overlap between the cluster Cu(1) z^2-y^2 band and the cluster Cu(2) x^2-y^2 band of **6.1a**, **8.1a**, and **9a** is 0.023, 0.069, and 0.058 eV. Some models (**3.1a**, **4a**, **5a**, and **6.2a**) with more than one unit along the *a*- and *b*-directions have almost zero band gap between two cluster bands near the highest occupied energy level. Figure 6 shows that the band gap between the bottom of the cluster x^2-y^2 Cu(2) band and the top of the cluster z^2 Cu(1) band for the charged model clusters representing $YBa_2Cu_3O_6$ rapidly decreases with increasing the size of the charged model clusters from one unit to (3×3×1) units [denoted ($a\times b\times c$) directions]. But the band gaps between the cluster x^2-y^2 Cu(2) band and the cluster z^2 Cu(1) band of all clusters representing $YBa_2Cu_3O_6$ are over 1.0 eV. The results represent the important role of the CuO_3 chains for the molecular energy level diagrams of the charged model clusters. Figures 7 shows that the energy gap (E_g) between the bottom of the cluster z^2-y^2 Cu(1) band and the highest-energy occupied level of the cluster x^2-y^2 Cu(2) band, for the charged model clusters representing $YBa_2Cu_3O_7$, is heavily dependent upon the size of the clusters along the *b*-direction. Here the E_g(eV) between the bottom of the cluster z^2-y^2 Cu(1) band and the highest-energy occupied level of the cluster x^2-y^2 Cu(2) band for **3.1a**, **5a**, **6.1a**, **8.1a**, and **9a** with three or more units along the *b*-direction is about 0.2 while the others have some values within the range of $0.25\leq E_g\leq 0.50$.

In this paper we present the comparative study for electron population analysis on one unit model of the most symmetric site for each charged model clusters with a Mulliken population analysis.[20] Afterward we call this chosen unit model as the central unit. Figure 8 shows that with the increment of size of charged model clusters representing $YBa_2Cu_3O_7$, the valence electron populations (VEP's) at Cu(2) of the central unit in **9a** are noticeably increased and at Cu(2) in the others are monotonously increased while those at Cu (1) are almost unchanged. Here the lack of coordinate satu-

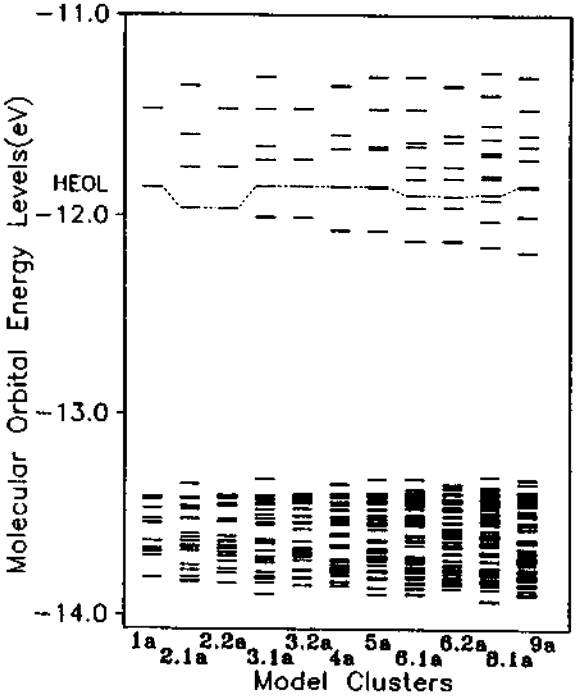

Figure 3. Molecular orbital energy level diagrams for the charged model clusters **1a-9a** as determined by EHTMO cluster calculations.

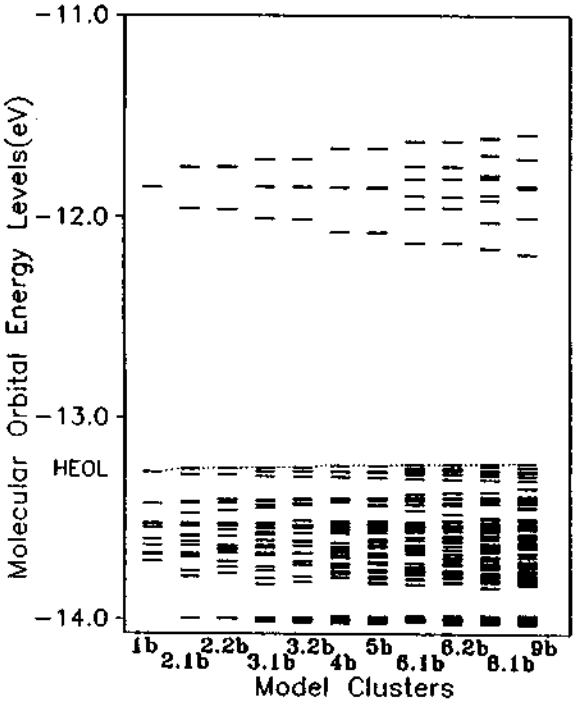

Figure 4. Molecular orbital energy level diagrams for the charged model clusters **1b-9b** as determined by EHTMO cluster calculations.

ration for the exterior atoms of the charged model clusters may imply the fact that some electrons in the bulk material would be related to the bonding interations with the atoms that are absent in the cluster, which are free to migrate to the central atom. But the comparison Figure 8 with 9

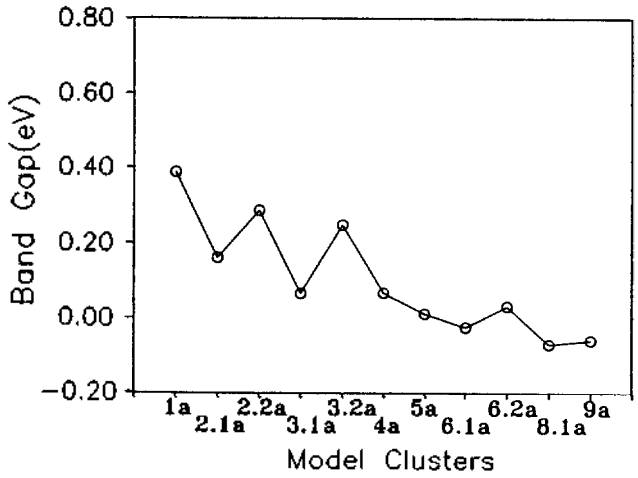

Figure 5. Band gap between the bottom of the cluster z^2-y^2 Cu(1) band and the top of the cluster x^2-y^2 Cu(2) band for the charged model clusters representing $YBa_2Cu_3O_7$.

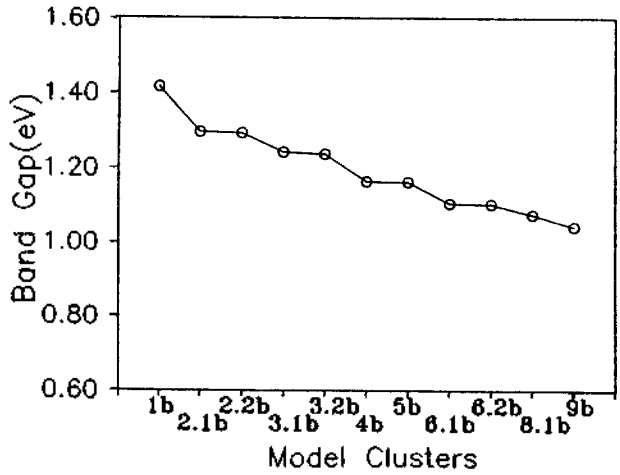

Figure 6. Band gap between the bottom of the cluster x^2-y^2 Cu(2) band and the top of the cluster z^2 Cu(1) band for the charged model clusters representing $YBa_2Cu_3O_6$.

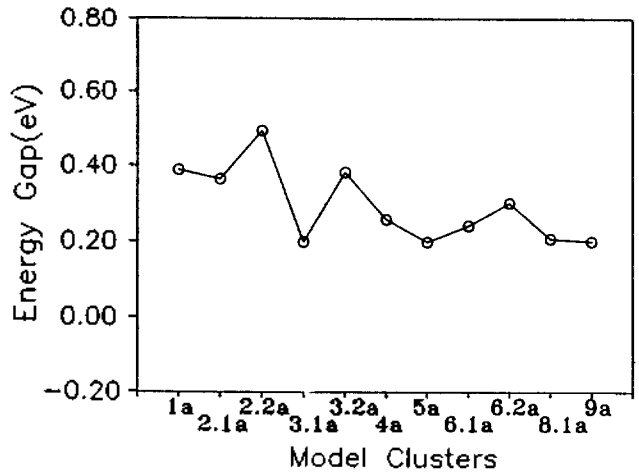

Figure 7. Energy gap between the bottom of the cluster z^2-y^2 Cu(1) band and the highest-energy occupied level of the cluster x^2-y^2 Cu(2) band for the charged model clusters representing $YBa_2Cu_3O_7$.

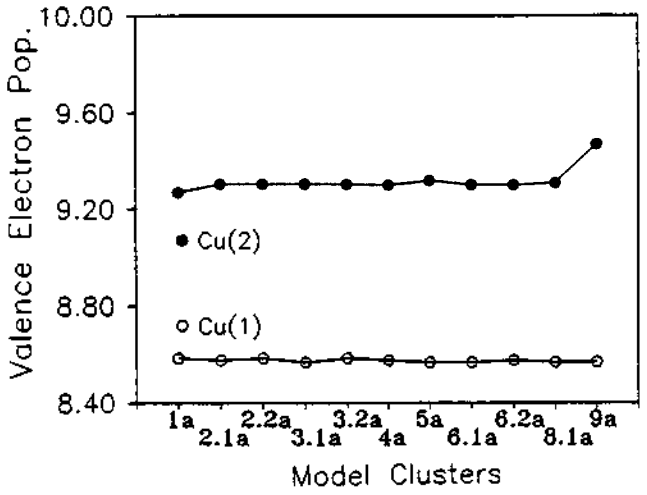

Figure 8. Valence electron populations for Cu(1) and Cu(2) *d* orbitals in the charged model clusters representing $YBa_2Cu_3O_7$.

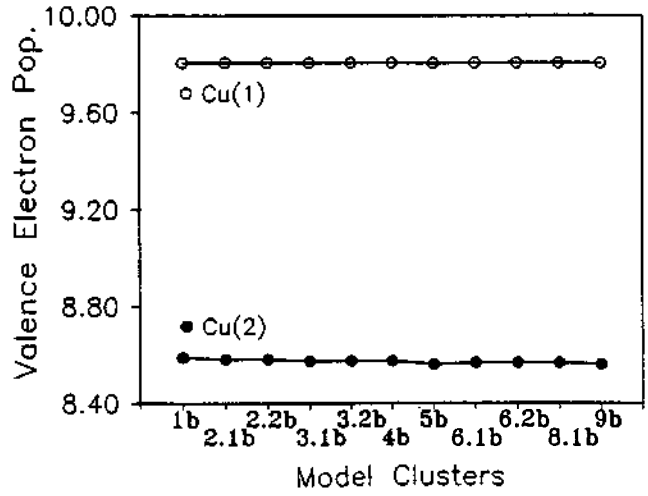

Figure 9. Valence electron populations for Cu(1) and Cu(2) *d* orbitals in the charged model clusters representing $YBa_2Cu_3O_6$.

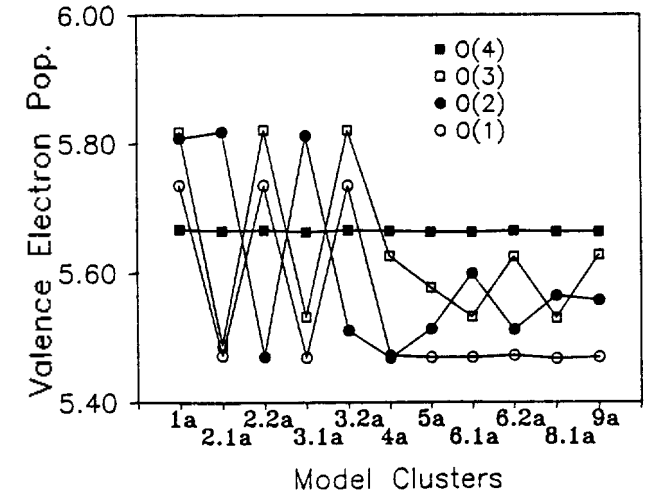

Figure 10. Valence electron populations for each site of oxygen 2*p* orbitals in the charged model clusters representing $YBa_2Cu_3O_7$.

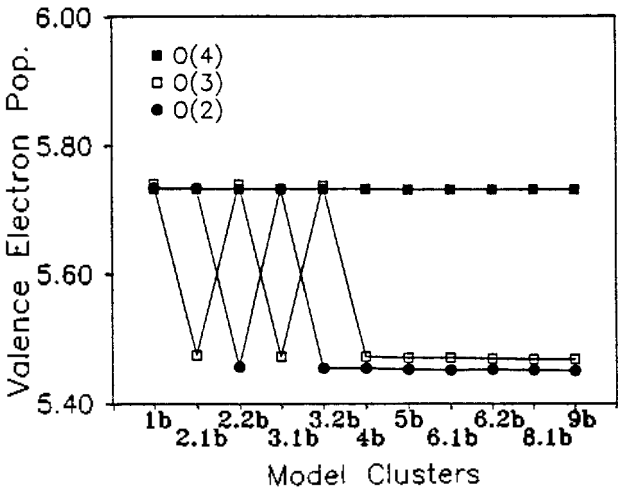

Figure 11. Valence electron populations for each site of oxygen 2*p* orbitals in the charged model clusters representing $YBa_2Cu_3O_6$.

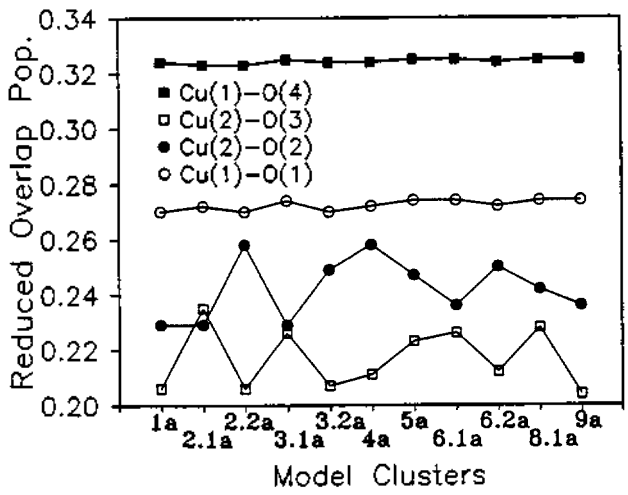

Figure 12. Reduced overlap populations for the charged model clusters representing $YBa_2Cu_3O_7$.

gives that the VEP's at Cu(2) *d* orbitals of the central unit in **9a** arises from the interaction between the central Cu(2) and the near-, second-, third-, ----- neighbor atomic wavefunctions. Thus the results suggest that the oxidation state of Cu(2) is susceptible to the size change of the charged model clusters and the environment condition representing $YBa_2Cu_3O_7$ while the state of Cu(1) is not sensitive. The VEP's for O(2) and O(3) sites of O 2*p* orbitals in the CuO_2 layers are seriously dependent upon the size change of the charged model clusters representing $YBa_2Cu_3O_7$ shown in Figure 10, while the VEP's shown in Figure 11 are almost same when the size of the charged model clusters represents $YBa_2Cu_3O_6$ ≥**4b**.

On the assumption that the cluster is equivalent to the bulk specimen, the size of the charged model clusters which is just large enough to yield the bulk value of a particular property is very important. It may be inferred from Figures 10 and 11 as follows: for $YBa_2Cu_3O_7$, the proper cluster size ≥**9a**; for $YBa_2Cu_3O_6$, the proper cluster size ≥**4b**.

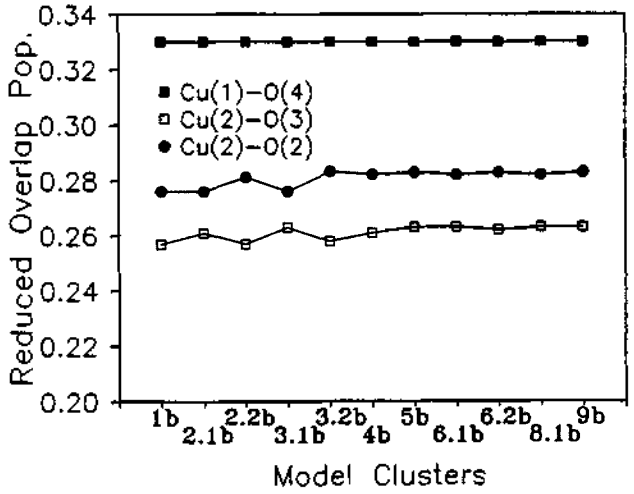

Figure 13. Reduced overlap populations for the charged model clusters representing $YBa_2Cu_3O_6$.

As shown in Figure 12 the reduced overlap populations (ROP's) of the charged model clusters representing superconducting $YBa_2Cu_3O_7$ show that ROP's of Cu(1)-O(1) and Cu (1)-O(4) at each central unit of the charged model clusters are almost same, but ROP's of Cu(2)-O(2) and Cu(2)-O(3) at each central unit of the charged model clusters are very susceptible to the size change of the charged model clusters and the environment condition. As shown in Figure 13 ROP's at each central units of the charged model clusters representing insulator $YBa_2Cu_3O_6$ show that each ROP's of each Cu-O bonds is almost same when the model cluster size $\geq$**4b**. Also, VEP's at each central units of the charged model clusters with the CuO_3 chains are more localized than those without the CuO_3 chains. Thus, the calculated results of the charged model clusters suggest that the Cu-O bonds in the CuO_2 layers for the charged model clusters with the CuO_3 chains are weaker than those without the CuO_3 chains.

The above results for VEP's and ROP's suggest that when one apply the band calculation with the tight binding method to the electronic structure of the high-T_c superconductor $YBa_2Cu_3O_{7-x}$ material, care should be needed to neglect moderate-to-strong hybridization it may contain large number of orbitals on second-, third-, ---neighbors.

Discussion and Concluding Remarks

The band gap between the bottom of the cluster z^2-y^2 Cu (1) band and the top of the cluster x^2-y^2 Cu(2) band, and the energy gap between the bottom of the cluster z^2-y^2 Cu(1) band and the highest-energy occupied level of the cluster x^2-y^2 Cu(2) band show the same pattern as the band electronic structures[12b,18,19] of the orthogonal phases of the high-T_c superconductor, $YBa_2Cu_3O_7$. Here the calculated results of the charged model clusters representing superconductor $YBa_2Cu_3O_7$ and insulator $YBa_2Cu_3O_6$ show the metallic properties, thus showing the limitation of extended Hückel method to the strong electron-electron (or electron-phonon) interaction system. Molecular energy level diagrams and electron population analyses show that the electronic structures of the CuO_2 layers are very susceptible, with increasing the unit cluster of the CuO_3 chain along the *b*-direction and along both the *a*- and *b*-directions.

The valence electron analysis of the charged model clusters representing superconductor $YBa_2Cu_3O_7$ shows that the Cu-O-Cu-O-Cu linkage in the CuO_2 layers along the *a*- and *b*-direction and the Cu(2)-O(4)-Cu(1)-O(4)-Cu(2) linkage along the *c*-direction seem to have some important consequence because the electron populations of each atom in the CuO_2 layers are very sensitive to the lattice coupling, which can be inferred from our results. The results of the charged model clusters without the CuO_3 chains representing insulator $YBa_2Cu_3O_6$ show that the electron popultions of the Cu-O-Cu-O-Cu linkage in the CuO_2 layers is not susceptible of the lattice environment. In conclusion, our results suggest that the CuO_3 chains along the *b*-direction play an important role in affecting the electronic structures of CuO_2 layers, thus showing important coupling between the layers and chains. To summarize this, in turn, the CuO_3 chains along the *b*-direction may yield to affect the conducting and superconducting properties of CuO_2 layers in $YBa_2Cu_3O_{7-x}$ system through cooperative electronic coupling of CuO_3 chains with the CuO_2 layers.

Acknowledgement. This work was partially supported by the Korea Science and Enginneering Foundation in 1990.

References

1. M. K. Wu, J. R. Ashburn, C. J. Torng, P. H. Hor, R. L. Meng, L. Gao, Z. J. Huang, Y. Q. Wang, and C. W. Chu, *Phys. Rev. Lett.*, **58**, 908 (1987).
2. J. M. Tarascon, L. H. Greene, W. R. McKinnon, and G. W. Hull, *Phys. Rev.*, **B35**, 7115 (1987).
3. G. Deutcher, "*Advanced in Superconductivity*", T. Kitazawa and T. Ishiguro, ed., p. 383. Springer-Verlag, Tokyo (1989).
4. A. W. Sleight, *Science*, **242**, 1519 (1988).
5. M. A. Beno, L. Soderholm, D. W. Capone, D. G. Hinks, J. D. Jorgensen, I. K. Suhuller, C. U. Segre, K. Z. Hang, and J. D. Grace, *Appl. Phys. Lett.*, **51**, 57 (1987).
6. J. D. Jorgensen, M. A. Beno, D. G. Hinks, L. Soderholm, K. J. Volin, R. L. Hilterman, J. D. Grace, I. K. Schuller, C. U. Segre, K. Zhang, and M. S. Kleefisch, *Phys. Rev.*, **B36**, 3608 (1987).
7. F. Beech, S. Miraglia, A. Santoro, and R. S. Roth, *Phys. Rev.*, **B35**, 8778 (1987).
8. M. François, E. Walker, J. L. Jorda, K. Yvon, and P. Fischer, *Solid State Commun.*, **63**, 1149 (1987).
9. (a) J. M. Tarascon, W. R. McKinnon, L. H. Greene, G. W. Hull, and E. M. Vogel, *Phys. Rev.*, **B36**, 226 (1987); (b) F. Zuo, B. R. Patton, D. L. Cox, S. I. Lee, Y. Song, J. P. Golben, X. D. Chen, S. Y. Lee, Y. Cao, Y. Lu, J. R. Gaines, J. C. Garland, and A. J. Epstein, *Phys. Rev.*, **B36**, 3603 (1987).
10. (a) M. Onoda, S. Shamoto, M. Sato, and S. Hosoya, *Jpn. J. Appl. Phys.*, **26**, L363 (1987); (b) J. M. Tarascon, L. H. Greene, W. R. McKinnon, G. W. Hull, and T. H. Gebalie, *Science*, **235**, 1373 (1987).
11. (a) G. Xiao, M. Z. Cieplak, A. Gavrin, F. H. Streitz, A. Bakhshai, and C. L. Chien, *Phys. Rev. Lett.*, **60**, 1446 (1988); (b) Q. Song, B. P. Clayman, and S. Gygax, *Physica C*, **165**, 328 (1990).
12. For reviews, see: (a) A. W. Sleight, M. A. Subramanian,

and C. C. Torardi, *Mater. Res. Bull.*, **14**, 45 (1989); (b) W. E. Pickett, *Rev. Modern Phys.*, **61**, 433 (1989).
13. D. L. Kaiser, F. Holtzberg, M. F. Chisholm, and T. K. Worthington, *J. Cryst. Growth*, **85**, 593 (1987).
14. H. Schmidt, E. Burkhardt, B. N. Sun, and J. P. Rivera, *Physica C*, **157**, 555 (1989).
15. U. Welp, R. Bhadra, J. Z. Liu, and M. Grimsditch, *Physica C*, **161**, 345 (1989).
16. R. H. Summerville and R. Hoffmann, *J. Am. Chem. Soc.*, **98**, 7240 (1976).
17. L. A. Curtiss, T. O. Brun, and D. M. Gruen, *Inorg. Chem.*, **27**, 1421 (1988).
18. S. Massida, J. Yu, A. J. Freeman, and D. D. Koelling, *Phys. Lett.*, **A122**, 198 (1987).
19. M.-H. Whangbo, M. Evain, M. A. Beno, U. Geiser, and J. M. Williams, *Inorg. Chem.*, **26**, 2566 (1987).
20. S. P. McGlynn, L. G. Vanquickenborine, M. Kinoshita, and D. G. Carroll, "Introduction to Applied Quantum Chemistry", Holt, Rinehart and Winston, Inc., New York (1972).

Reaction of 2,2'-Biphenoxyborane in Tetrahydrofuran with Selected Organic Compounds Containing Representative Functional Groups

Jin Soon Cha, Jong Mi Kim, Jae Cheol Lee, and Hyung Soo Lee*

Department of Chemistry, Yeungnam University, Gyongsan 712-749
**Department of Chemistry Education, Hyosung Women's University, Hayang 713-702.* *Received April 30, 1991*

The approximate rates and stoichiometry of the reaction of excess 1,3,2-biphenyldioxaborepin [2,2'-biphenoxyborane (BPB)] with selected organic compounds containing representative functional groups under the standardized conditions (tetrahydrofuran, hydride to compound being 4 : 1, room temperature) was examined in order to define the characteristics of the reagent for selective reductions and compare its reducing power with those of other substituted boranes. The results indicate that BPB is unique and the reducing power is much stronger than that of other dialkoxyboranes, such as catecholborane and di-*s*-butoxyborane. BPB reduces aldehydes, ketones, quinones, lactones, tertiary amides, and sulfoxides readily. Carboxylic acids, anhydrides, esters, and nitriles are also reduced slowly. However, the reactions of acid chlorides, epoxides, primary amides, nitro compounds, and disulfides with this reagent proceed only sluggishly.

Introduction

Catecholborane (1,3,2-benzodioxaborole) has appeared to be a very useful hydroborating agent.[1] The usefulness of catecholborane as a hydroborating agent is enhanced by the fact that the reagent can tolerate a number of functional groups under hydroboration conditions, because catecholborane is a mild reducing agent.[1a,b] Similarly, di-*s*-butoxyborane appears to be an extremely mild, even milder than catecholborane, reducing agent.[2] With the exception of simple aldehydes, most functional groups studied are inert toward this reagent.

This uniqueness of stable dialkoxyboranes attracted us. We became to believe that the systematic study on the hydroboration and reduction reactions of various dialkoxyboranes will make a broad spectrum of their reducing and hydroborating properties which, in turn, provide useful applications. Therefore, we decided to explore the reducing characteristics of 1,3,2-biphenyldioxaborepin [2,2'-biphenoxyborane (BPB) **1**], a new stable cyclic dialkoxyborane,[4] systematically.

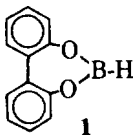

1

Results and Discussion

Preparation and Stability of the Reagent. 2,2-Biphenoxyborane (BPB), **1**, is readily prepared by the reaction of 2,2'-biphenol and borane in THF at −10℃ (Eq. 1).

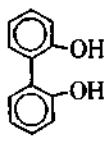

$$+ BH_3\cdot THF \xrightarrow[-10^\circ]{THF} \mathbf{1} + 2H_2\uparrow \qquad (1)$$

BPB is quite stable, similar to the stability of catecholborane and 4,4,6-trimethyl-1,3,2-dioxaborinane. We could not detect any significant change in B-11 NMR spectra and in hydride concentration for 6 months at room temperature.

Procedure for Rate and Stoichiometry Studies. The general procedure adopted in this study involved preparation of a reaction mixture of BPB (0.5 M, 0.5 M in hydride) and the compound (0.125 M) under study in THF at room temperature. The solution was maintained at room temperature. In some cases where the hydride-to-compound ratio of 4 : 1 is not adequate for complete reduction, the hydride concentration was maintained constant, but the concentration of compound, was reduced to give a higher ratio. Hydrogen evolution, following addition of the compound to be examined to the reagent, was measured. A blank reaction was run un-